

## A Highly Efficient Dye-sensitized Solar Cell Based on a Triarylamine-functionalized Ruthenium Dye

Zhengzhe Jin,<sup>1</sup> Hideki Masuda,\*<sup>1</sup> Noriyo Yamanaka,<sup>2</sup> Masaki Minami,<sup>2</sup> Tsutomu Nakamura,<sup>2</sup> and Yoshinori Nishikitani<sup>2</sup>

<sup>1</sup>Department of Applied Chemistry, Graduate School of Engineering, Nagoya Institute of Technology, Showa-ku, Nagoya 466-8555

<sup>2</sup>Central Technical Research Laboratory, Nippon Oil Corporation, Yokohama 231-0815

(Received August 28, 2008; CL-080821; E-mail: masuda.hideki@nitech.ac.jp)

A new ruthenium dye with an electron donating triarylamine ligand, J8, has been synthesized as a highly efficient sensitizer for a dye-sensitized solar cell, giving an overall conversion efficiency of 7.2% in the preliminary tests.

Dye-sensitized solar cells (DSSCs) based on mesoporous nanocrystalline TiO<sub>2</sub> films have attracted intensive interest for scientific and industrial applications due to their high photo-to-electricity conversion efficiency and low production cost.<sup>1</sup> Although numerous sensitizers such as metal-free organic dyes<sup>2</sup> and non-ruthenium metal dyes<sup>3</sup> have been employed, the best energy conversion efficiency of up to 11% was achieved only by using ruthenium dyes, such as N3, N719, and black dye<sup>4</sup> in standard global air mass 1.5 sunlight. To further increase the efficiency of these cells, much effort has been directed toward the development of highly efficient solar cells based on ruthenium dyes.<sup>5</sup> A recent strategy for identification of new ruthenium dyes is to replace one of the 4,4'-dicarboxylic acid-2,2'-bipyridine (dcbpy) ligands of N3 with a highly conjugated ancillary ligand. This strategy has two main disadvantages: (i) one is a relatively low adsorption of dye molecules onto the TiO<sub>2</sub> particles, and (ii) another is that the electron excited on the highly conjugated ancillary ligand is not effectively injected into the electrode because it is not directly connected to the TiO<sub>2</sub> particles.<sup>6</sup> These cause a lower conversion efficiency (<11%) of the DSSCs.

Here, we introduced a new triarylamine derivative as the highly conjugated ancillary ligand, which has attracted great interest because of excellent hole-transport capabilities.<sup>7</sup> The organic dyes including the triarylamine moieties are also known to exhibit highly efficient conversion of solar energy into electricity.<sup>8</sup> Based on the above considerations, we have designed a novel ruthenium dye J8 (see Inset of Figure 1) consisting of

dcbpy (which acts as the electron acceptor and anchoring ligand), thiocyanato ligands, Ru metal acting as an electron donor, and a triarylamine ligand as an electron donor. Furthermore, the methoxy and *tert*-butyl substituents on arylamine not only are capable of tuning the HOMO and LUMO energy levels of the dyes and provide directionality to the efficient electron transfer from the excited dye to the TiO<sub>2</sub> conduction band<sup>9</sup> but also stabilize device performance under long-term light soaking and thermal stress.<sup>10</sup>

J8 was prepared in a one-pot synthesis, and characterized using NMR, ESI-TOFMS, and FTIR spectroscopies and elemental analysis.<sup>11</sup> The absorption spectrum of J8 is shown in Figure 1. The spectrum is dominated by two absorption features at 381 nm ( $14.7 \times 10^3 \text{ M}^{-1} \text{ cm}^{-1}$ ) and 514 nm ( $9.6 \times 10^3 \text{ M}^{-1} \text{ cm}^{-1}$ ) in the visible region and by a strong feature at 300 nm ( $49.4 \times 10^3 \text{ M}^{-1} \text{ cm}^{-1}$ ) in the UV region. The absorption spectrum of J8 adsorbed on TiO<sub>2</sub> electrodes is similar to the corresponding solution spectrum, although they exhibit a red shift due to the interaction of the anchoring groups with the surface titanium ions.

The ionization potential of J8 on TiO<sub>2</sub> electrode was measured on a Riken Keiki AC-2 instrument. The ionization potential is  $-5.1 \text{ eV}$ , which is  $0.3 \text{ eV}$  more negative than the potential of the iodide/triiodide redox couple in the electrolyte, providing a large thermodynamic driving force for sensitizer regeneration by iodide. The emission maxima of J8 appeared at 712 nm. The excited-state oxidation potential derived from the ionization potential and the zero-zero excitation energy is  $-3.3 \text{ eV}$ , which is  $0.6 \text{ eV}$  more positive than the TiO<sub>2</sub> conduction band, providing an efficient electron transfer from the excited dye to the TiO<sub>2</sub> conduction band.

To gain insight into the geometric, electronic, and optical properties of the ruthenium sensitizers, DFT and TD-DFT calculations have been intensively investigated. The molecular orbital energy diagrams calculated for J8 are shown in Figure 2. The three highest occupied molecular orbitals (HOMO, HOMO-1, and HOMO-2) have essentially ruthenium  $t_{2g}$  character with a significant contribution originating from the NCS ligand orbitals, which are mixed in an antibonding arrangement with the metal states. The three lowest unoccupied molecular orbitals (LUMO, LUMO+1, and LUMO+2) are localized homogeneously on the dcbpy anchoring ligand. The excited electrons are directly transferred to TiO<sub>2</sub> through these orbitals. Similar locations of LUMO, LUMO+1, and LUMO+2 are also found in N3, N719, and black dye.<sup>12</sup> However, for the other Ru complexes, the three lowest unoccupied molecular orbitals are localized on the two different ligands.<sup>13</sup> A comparison between calculated and experimental absorption spectra of J8 is shown in Figure 1. Surprisingly, the calculated and experimentally determined ab-

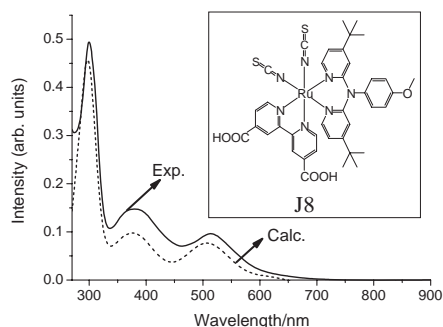


**Figure 1.** Comparison of the calculated (dashed line) and experimental (solid line) absorption spectra of J8. The inset is the molecular structure of J8.

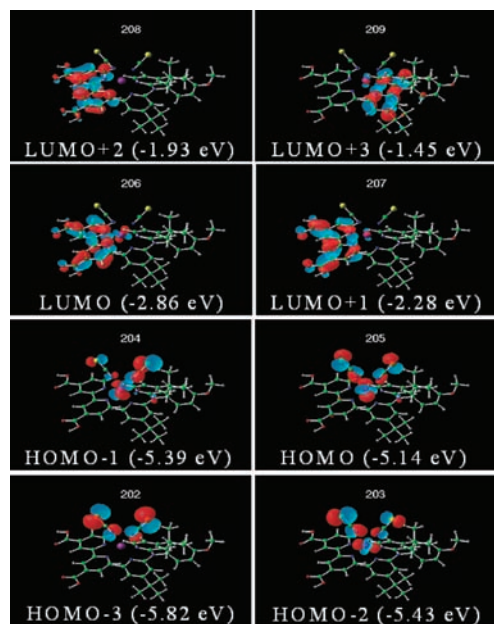


**Figure 2.** Isodensity surface plots and MO energies of the frontier orbitals of J8.

sorption positions and their relative intensities are in good agreement. The TD-DFT calculation predicts the existence of two absorption bands in the visible region originating from the MLCT transitions from Ru(NCS) to the anchoring ligand dc bpy, through which the excited electrons are directly transferred to TiO<sub>2</sub>.

The inset of Figure 3 shows the incident monochromatic photo-to-current conversion efficiency (IPCE) for J8. The IPCE data of J8 exceeds 70% in a spectral range from 395 to 645 nm, and the IPCE data plotted as a function of excitation wavelength exhibits a strikingly high efficiency of 86.5%. The photocurrent density–photovoltage curve is shown in Figure 3 and the detailed device parameters are listed in Table 1. Under standard global AM 1.5 solar conditions, the J8-sensitized solar cell produces a short circuit current density ( $J_{sc}$ ) of 17.3 mA cm<sup>-2</sup>, an open-circuit photo-voltage ( $V_{oc}$ ) of 640 mV, and a fill factor ( $FF$ ) of 0.65, corresponding to an overall conversion efficiency ( $\eta$ ) of

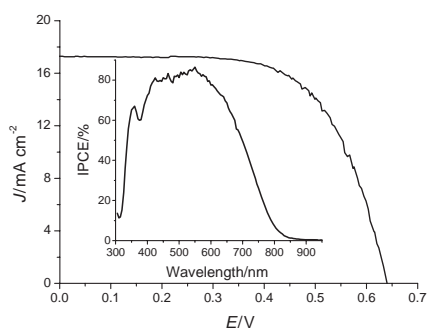


**Figure 3.** Photocurrent density–photovoltage curve of J8 under AM 1.5 G radiation (100 mW cm<sup>-2</sup>) (0.6 M 2,3-dimethyl-1-propylimidazolium iodide, 20 mM iodine, 0.1 mM LiI, and 0.5 M 4-*tert*-butylpyridine in acetonitrile). The inset is the incident photo-to-current conversion efficiency spectrum for dye-sensitized solar cells based on J8.

**Table 1.** Photovoltaic performance of the dye-sensitized solar cell based on J8, as compared to the N719 dye

Dye	$V_{oc}/V$	$J_{sc}/\text{mA cm}^{-2}$	$FF$	$\eta/\%$
J8	0.64	17.3	0.65	7.2
N719	0.66	17.5	0.70	8.0

7.2%. These values are close to those of the N719-sensitized solar cell. Further optimization of the cell parameters to take the full potential of these new sensitizers is underway.

This work was supported by a Grant-in-Aid for Scientific Research from the Ministry of Education, Culture, Sports, Science and Technology, to which our thanks are due.

#### References and Notes

- 1 M. Grätzel, *Nature* **2001**, 414, 338.
- 2 a) T. Horiuchi, H. Miura, K. Sumioka, S. Uchida, *J. Am. Chem. Soc.* **2004**, 126, 12218. b) S. Ito, S. M. Zakeeruddin, R. Humphry-Baker, P. Liska, R. Charvet, P. Comte, M. K. Nazeeruddin, P. Péchy, M. Takata, H. Miura, S. Uchida, M. Grätzel, *Adv. Mater.* **2006**, 18, 1202.
- 3 a) A. Islam, H. Sugihara, K. Hara, L. P. Singh, R. Katoh, M. Yanagida, Y. Takahashi, S. Murata, H. Arakawa, *Inorg. Chem.* **2001**, 40, 5371. b) E. A. M. Geary, L. J. Yellowlees, L. A. Jack, I. D. H. Oswald, S. Parsons, N. Hirata, J. R. Durrant, N. Robertson, *Inorg. Chem.* **2005**, 44, 242.
- 4 a) M. K. Nazeeruddin, A. Kay, I. Rodicio, R. Humphry-Baker, E. Müller, P. Liska, N. Vlachopoulos, M. Grätzel, *J. Am. Chem. Soc.* **1993**, 115, 6382. b) M. K. Nazeeruddin, P. Péchy, T. Renouard, S. M. Zakeeruddin, R. Humphry-Baker, P. Comte, P. Liska, L. Cevey, E. Costa, V. Shklover, L. Spiccia, G. B. Deacon, C. A. Bignozzi, M. Grätzel, *J. Am. Chem. Soc.* **2001**, 123, 1613.
- 5 M. Grätzel, *Bull. Jpn. Soc. Coord. Chem.* **2008**, 51, 3.
- 6 C.-Y. Chen, S.-J. Wu, C.-G. Wu, J.-G. Chen, K.-C. Ho, *Angew. Chem., Int. Ed.* **2006**, 45, 5822.
- 7 a) Y. Shirota, *J. Mater. Chem.* **2005**, 15, 75. b) Z. Ning, Z. Chen, Q. Zhang, Y. Yan, S. Qian, Y. Cao, H. Tian, *Adv. Funct. Mater.* **2007**, 17, 3799.
- 8 S. Hwang, J. H. Lee, C. Park, H. Lee, C. Kim, C. Park, M.-H. Lee, W. Lee, J. Park, K. Kim, N.-G. Park, C. Kim, *Chem. Commun.* **2007**, 4887.
- 9 M. K. Nazeeruddin, Q. Wang, L. Cevey, V. Aranyos, P. Liska, E. Figgemeier, C. Klein, N. Hirata, S. Koops, S. A. Haque, J. R. Durrant, A. Hagfeldt, A. B. P. Lever, M. Grätzel, *Inorg. Chem.* **2006**, 45, 787.
- 10 D. Kuang, S. Ito, B. Wenger, C. Klein, J.-E. Moser, R. Humphry-Baker, S. M. Zakeeruddin, M. Grätzel, *J. Am. Chem. Soc.* **2006**, 128, 4146.
- 11 Data for J8: <sup>1</sup>H NMR (600 MHz, CD<sub>3</sub>OD + NaOD):  $\delta$  9.41 (d,  $J = 5.8$  Hz, 1H), 9.00 (s, 1H), 8.97 (s, 1H), 8.91 (d,  $J = 6.3$  Hz, 1H), 8.47 (d,  $J = 5.8$  Hz, 1H), 8.12 (d,  $J = 5.8$  Hz, 1H), 7.82 (d,  $J = 5.8$  Hz, 1H), 7.68 (d,  $J = 8.9$  Hz, 2H), 7.34 (d,  $J = 6.3$  Hz, 1H), 7.29 (d,  $J = 8.9$  Hz, 2H), 7.11 (s, 1H), 7.00 (d,  $J = 6.5$  Hz, 1H), 6.76 (s, 1H), 6.63 (d,  $J = 6.5$  Hz, 1H), 3.96 (s, 3H), 3.29 (t,  $J = 8.3$  Hz, 4H), 1.72 (m, 4H), 1.43 (m, 4H), 1.30 (s, 9H), 1.04 (m, 15H). FTIR: 2108 (–NCS), 1719 (–COOH). ESI-MS (CH<sub>3</sub>OH + TBAOH):  $m/z$  424.3 [M – 2H]<sup>2+</sup>. Anal. Calcd for C<sub>39</sub>H<sub>39</sub>N<sub>7</sub>O<sub>5</sub>RuS<sub>2</sub>·2.75H<sub>2</sub>O·0.5TBA: C, 55.25; H, 6.17; N, 10.28%. Found: C, 55.36; H, 5.95; N, 10.07%.
- 12 a) M. K. Nazeeruddin, F. D. Angelis, S. Fantacci, A. Selloni, G. Viscardi, P. Liska, S. Ito, B. Takeru, M. Grätzel, *J. Am. Chem. Soc.* **2005**, 127, 16835. b) S. Ghosh, G. K. Chaitanya, K. Bhanuprakash, M. K. Nazeeruddin, M. Grätzel, P. Y. Reddy, *Inorg. Chem.* **2006**, 45, 7600.
- 13 M. K. Nazeeruddin, T. Bessho, L. Cevey, S. Ito, C. Klein, F. D. Angelis, S. Fantacci, P. Comte, P. Liska, H. Imai, M. Grätzel, *J. Photochem. Photobiol., A* **2007**, 185, 331.